

IMP-1 inhibits renal cell carcinoma 786-O cell growth by targeting EphrinB2 signaling pathway

Juan Liu¹, Hong Shi^{2*}

¹Department of Oncology, The Weapons Industry of institutes of health, Xi'an, Shaanxi, China, ²Department of Oncology, Tangdu Hospital, The Airforce Military Medical University, Xi'an, Shaanxi, China

EphrinB2 plays a critical role in tumor growth. In this study, we studied the antitumor activity of imperatorin derivative IMP-1 in renal cell carcinoma (RCC) by regulating EphrinB2 pathway. Results showed that IMP-1 inhibited the proliferation of 786-O cells in a dose- and time-dependent manner. More importantly, knockdown and transfection of EphrinB2 altered the inhibitory effect of IMP-1 on the activity of 786-O cells. IMP-1 arrested 786-O cell cycle at G0/G1 phase by decreasing the expression of cyclin D1 and cyclin E. Moreover, IMP-1 regulated Bcl-2 family proteins' expression, thus inducing apoptosis of 786-O cells. IMP-1 down-regulated the expression of EphrinB2, Syntenin1 and PICK1. Then, IMP-1 decreased the phosphorylation of Erk1/2 and AKT. In all, IMP-1 could regulate the EphrinB2 pathway in order to inhibit 786-O cell growth by arresting the cell cycle at G0/G1 phase and inducing cell apoptosis. Thus, IMP-1 may present as a potential strategy for RCC treatment.

Keywords: Renal cell carcinoma. IMP-1. EphrinB2. Cell cycle. Cell apoptosis.

INTRODUCTION

Renal cell carcinoma (RCC) is one of the most common and fatal tumors of the urinary system (Liu *et al.*, 2020). The prognosis of advanced RCC is poor, and the 5-year survival rate is about 5%-10% (Li *et al.*, 2017). According to the histological characteristics, growth kinetics and histochemical characteristics of RCC, it can be divided into clear cell (75%), papillary (15-20%), and chromophobe (5%) (Gray, Harris, 2019). Nephrectomy is still an important intervention for localized RCC, but systematic therapy is the main treatment method for patients with relapsed or metastatic RCC after surgery (Posadas, Limvorasak, Figlin, 2017; Curtis, Cohen, Kluger, 2016). The recognized severe toxicity and relatively low response rate (5-27%) of this therapy has prompted people

to find more effective and less toxic treatment methods (Posadas, Limvorasak, Figlin, 2017).

Eph receptor tyrosine kinase and its plasma membrane-anchored Ephrin ligand play a key role in angiogenesis, cell proliferation, and cell migration in many different types of cancer cells and tissues (Zhu *et al.*, 2018). Eph receptors and Ephrin ligands bind and aggregate on the cell membrane, and transduce signals that regulate cell responses (Poliakov, Cotrina, Wilkinson, 2004). The interaction of Eph receptor and Ephrin ligand can lead to bidirectional signals, which are transmitted to both receptor-expressing cells (forward signal) and ligand-expressing cells (reverse signal) (Genander, Frisen, 2010). EphrinB2 is a transmembrane subclass ligand for Eph receptor tyrosine kinases. Its reverse signal transduction is mediated by the EphrinB2 cytoplasmic domain, which contains a PDZ binding motif and a tyrosine phosphorylation site, which can interact with signaling molecules (Dravis, Henkemeyer, 2011). Recent studies have shown that EphrinB2 reverse signaling pathway increases the proliferation and migration of EphrinB2-

*Correspondence: H. Shi. Department of Oncology, Tangdu Hospital. The Airforce Military Medical University. Xi'an, Shaanxi, 710038, China. E-mail: blogmm202010@163.com. Phone: +86-29-82656788. Fax: +86-29-82655451. ORCID: <https://orcid.org/0000-0002-3491-6127>

bearing cells (Ma *et al.*, 2017a; Ma *et al.*, 2017b). Emerging evidences show EphrinB2 could activate downstream signal transduction pathways such as PI3K/AKT and MEK/ERK pathways, thereby regulating cell cycle and apoptosis (Germain, Eichmann, 2010).

Uncontrolled cell proliferation caused by cell cycle demodulation is one of the most common changes in tumor development. The mammalian cell cycle is controlled by the cyclin-dependent kinases (CDKs) subfamily, and its activity is regulated by a variety of activating factors (Cyclins) and inhibitors (Ink4, Cip and Kip inhibitors) (Malumbres, Barbacid, 2009). Cyclins bind and activate their CDKs to promote the progression of cell cycle (Bonelli *et al.*, 2019). Thus, blocking the cell cycle is considered to be an effective strategy against cancer cells.

As a genetic program event, apoptosis is often altered and/or disrupted in cancer cells, leading to malignant tumors, metastasis, and chemoresistance (Messeha *et al.*, 2020). In order to resist apoptosis, cancer cells can up-regulate the expression of anti-apoptotic proteins such as Bcl-2 and Bcl-xl, or down-regulate the expression of pro-apoptotic proteins such as Bax and Bak (Messeha *et al.*, 2019).

Imperatorin is a plant secondary metabolite, belonging to coumarins, especially furanocoumarins. It has been proved that imperatorin causes vasodilation by inhibiting voltage-gated Ca^{2+} influx, receptor-mediated Ca^{2+} entry and endothelial-derived NO release, and reduces angiotensin-stimulated myocardial hypertrophy (Kozioł, Skalicka-Woźniak, 2016; Wu *et al.*, 2013). In this study, we investigate the anti-cancer activity of imperatorin derivative IMP-1 (Figure 1a) in RCC 786-O cells.

MATERIAL AND METHODS

Chemicals and reagents

Trypsin, dimethylsulfoxide (DMSO), and 3-(4,5-dimethylthiazol-2-yl)-2,5-diphenyl-2H-tetrazolium bromide (MTT) were from Sigma-Aldrich (St. Louis, MO, USA). RPMI 1640 and MEM medium were purchased from Sigma-Aldrich (St. Louis, MO, USA). RNase and propidium iodide (PI) were from Sigma-Aldrich (St. Louis, MO, USA). Annexin V-FITC apoptosis kit was

from Pioneer Biotechnology Co., Ltd (Xi'an, China). Protease and phosphatase inhibitor cocktail were from Roche (Roche Technology, Switzerland). Antibodies were from Cell Signaling (Boston, Massachusetts, USA). Anti-GAPDH antibody and rabbit anti-mouse IgG were from Santa Cruz Biotech (CA, USA). Enhanced Chemiluminescent (ECL) Plus Reagent was from Biotech Co., Ltd (Beijing, China). The RNAfast200 kit was purchased from Fastagen (Shanghai, China) and lipofectamine 2000 reagent was purchased from Invitrogen (Carlsbad, USA). PrimeScript RT Master Mix Perfect Real Time kit, SYBR® Premix Ex Taq™ II and a Thermal Cycle Dice Real time system were purchased from TaKaRa (DRR036A) biotechnology (Dalian, China). IMP-1 (purity>95%) was from Dr. Wang as a gift which was synthesized in his lab (He *et al.*, 2015).

Cell culture

Renal cancer cell lines (786-O, 769-P, and A498 cells) were provided by Shanghai Institute for Biological Sciences (Shanghai, China). 786-O and 769-P cells were cultured in RPMI 1640 medium containing 10% FBS. A498 cells were cultured in MEM medium containing 10% FBS. All cells were cultured in 37 °C with the saturated humidity of 5% CO_2 .

Cell proliferation assay

The cells (786-O: 1×10^4 cells/well, 769-P: 5×10^3 cells/well, A498: 5×10^3 cells/well) were inoculated in a 96-well plates in complete medium for 24 h. The cells were treated with IMP-1 at concentration gradient for 24 h, 48 h, 72 h. Then, the medium was moved out from each well and the prepared MTT solution was added for 4 h. The medium in the 96-well plates was cleaned and DMSO (150 μ L/well) was added. The absorbance was recorded at a wavelength of 490 nm and the inhibition ratio was calculated.

Flow cytometric analysis of cell cycle

The cells were plated in 6-well plates (2×10^5 cells/well) and treated with corresponding concentrations

of IMP-1 for 48 h. Then, cells were collected, washed, resuspended in PBS. After centrifuging (5 min, 1000 rpm), 1 mL of pre-cooled 70% ethanol was added and placed at -20 °C for washing three times with PBS. Cells were incubated with 1 mL RNase at room temperature (light-proof operation) for 30 min and then added with PI (25 µL). Finally, cells were detected by flow cytometer.

Hoechst staining assay

After treating cells with different concentrations of IMP-1 for 48 h, the cells plated in 6-well plates (1x10⁵ cells/well) were incubated with Hoechst 33258 at 37 °C for 10 min according to the instructions. Then the cells were examined using fluorescence microscope.

Flow cytometric analysis of apoptosis

The cells were plated in 6-well plates (1x10⁵ cells/well) and treated with corresponding concentrations of IMP-1 for 48 h. Then, cells were collected, washed, resuspended in PBS. According to the instructions of the apoptosis kit, the cells were treated with PI and Annexin V-FITC double staining at 4 °C in dark for 20 min. Then, cells were detected by flow cytometer.

Determination of mitochondrial transmembrane potential ($\Delta\psi_m$)

The cells were plated in 6-well plates (1x10⁵ cells/well) and treated with corresponding concentrations of IMP-1 for 48 h. Then, cells were collected, washed, resuspended in RPMI 1640 medium. Then, cells were incubated with 1 mM Rhodamine 123 at 37 °C away from light for 30 min. Cells were then washed with RPMI 1640 medium again, and the fluorescent intensity was measured using flow cytometer.

RT-PCR and quantitative real-time PCR

Total RNA was extracted from cultured cells using the RNAfast200 kit according to the manufacturer's protocol. The total RNA (1 µg) was reversely transcribed in 20 µL reaction solution using the Revert AIDTM first

strand cDNA synthesis kit. Real-time PCR was performed using SYBR® Premix Ex Taq™ II and a Thermal Cycle Dice Real time system. Reaction volumes were 25 µL, containing 2 µL cDNA (50 ng/µL) and 100 µM of each pair of primers and SYBR® Premix Ex Taq™ II. The relative amount of EphrinB2 mRNA was normalized and represented as the ratio of the EphrinB2 mRNA value to that of the β -actin gene. The result was analyzed using the manufacturer's program (Thermal Cycler Dice™ Real Time System). The primer sequences were as following:

β -actin forward primer:

5'-AGCGTGGCTACAGCTTCACC -3'

β -actin reverse primer:

5'-AAGTCTAGGGCAACATAGCACAGC -3'

EphrinB2 forward primer:

5'-TCATCTTCATCGTCATCATCATC-3'

EphrinB2 reverse primer:

5'-CTGTCCGCAGTCCTTAGC-3'

Melt curve analysis was performed at the end of each PCR to confirm the specificity of the PCR product. Threshold cycle (Ct) values of EphrinB2 in each sample were normalized with the β -actin expression. The ratio of EphrinB2 versus the corresponding β -actin of each sample was determined on the basis of the equation $EphrinB2/\beta\text{-actin} = 2^{Ct(\beta\text{-actin}) - Ct(EphrinB2)}$.

Western blot analysis

The cells were plated in 6-well plates (2x10⁵ cells/well) and treated with corresponding concentrations of IMP-1 for 48 h. The cells were washed with PBS, and lysed with RIPA lysis buffer at 4 °C for 30 min. The cells were centrifuged in a refrigerated centrifuge (12000 rpm, 10 min, 4 °C) and the supernatant was collected. The protein samples (30 µg) which was quantified by BCA, were denatured by boiling for 5 min and loaded onto the SDS-PAGE gel (10%). Then, the samples were transferred onto the PVDF membrane in an ice bath. The PVDF membranes were washed 4 times with

1×TBST (5 min) and blocked in 10% non-fat milk for 2 h. Then the membranes were incubated with the primary antibody at 4 °C overnight. The membranes were washed 4 times with TBST (5 min) and then were incubated with secondary antibody at 37 °C for 1 h. The proteins on the membranes were detected by using ECL kit. An automatic chemiluminescence image processing system was used for photographing.

Plasmid and siRNA transfection

Exponentially growing 786-O cells were cultured until reaching 30%-50% confluence, and were transfected with EphrinB2 siRNA and Ephrin-B2-overexpression plasmids using Lipofectamine 2000 according to the manufacture's instruction. The ratio of Lipofectamine 2000 (μL) to EphrinB2 plasmid (μg) was 2:1.

Statistical analysis

Data are presented as the mean ± standard error of the mean and statistical analysis was performed using

analysis of variance. $P < 0.05$ was considered to indicate a statistically significant difference.

RESULTS

IMP-1 suppresses renal cell carcinoma 786-O cell growth

MTT assay was used to investigate the inhibitory effect of IMP-1 on the proliferation of renal carcinoma cells (786-O, 769-P and A498 cells). 786-O cells were the most sensitive to IMP-1 among all the three renal carcinoma cells (Figure 1a, b). Results showed IMP-1 inhibited the proliferation of 786-O cells in a dose- and time-dependent manner (Figure 1c). And the IC_{50} values of IMP-1 in 786-O cells were 8.92, 3.84 and 2.83 μM for 24, 48 and 72 h, respectively.

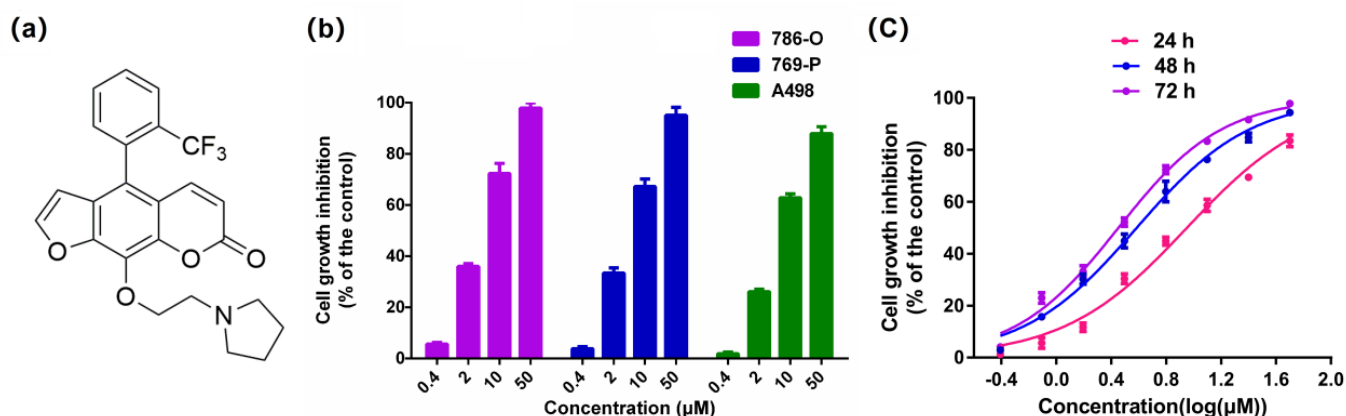


FIGURE 1 - The effect of IMP-1 on renal carcinoma cell growth. (a) The chemical structure of IMP-1. (b) Effect of IMP-1 on renal carcinoma cell growth at 48 h. (c) Effect of IMP-1 on 786-O cell growth at different time point. Cells were treated with various concentrations of IMP-1 for 24, 48 and 72 h and measured by MTT assay. Five wells were treated in each experiment and the data are presented as the mean ± standard error of the mean from three repeated experiments.

Effect of IMP-1 on cell cycle

The DNA of the cells were stained with PI and analyzed by flow cytometer to determine the effect

of IMP-1 on cell cycle. Compared with the control group, the proportion of G0/G1 phase cells in IMP-1 treatment group increased significantly, while the proportion of S phase cells decreased significantly.

The percentage of cells accumulated in the G0/G1 phase was 20.41, 23.13, 32.35 and 44.49% following treatment with IMP-1 concentrations of 0, 0.78, 1.56 and 3.12 μM , respectively. The decrease in the number of S phase cells was 77.78, 73.29, 67.65 and 55.51% with IMP-1 concentrations of 0, 0.78, 1.56 and 3.12 μM , respectively. These results indicated that IMP-1 mediated 786-O cell growth by inducing partial G0/G1 phase cell cycle arrest (Figure 2a).

Effects of IMP-1 on cell cycle regulatory molecules

The expression of cell cycle regulatory protein molecules were detected by western blot assay during treatment with IMP-1 for 48 h. IMP-1 did not affect the expression of CDC2, CDK2, Cyclin A2 and Cyclin B1. However, IMP-1 decreased Cyclin D1 and Cyclin E expression in a dose-dependent manner with increasing concentrations (Figure 2b).

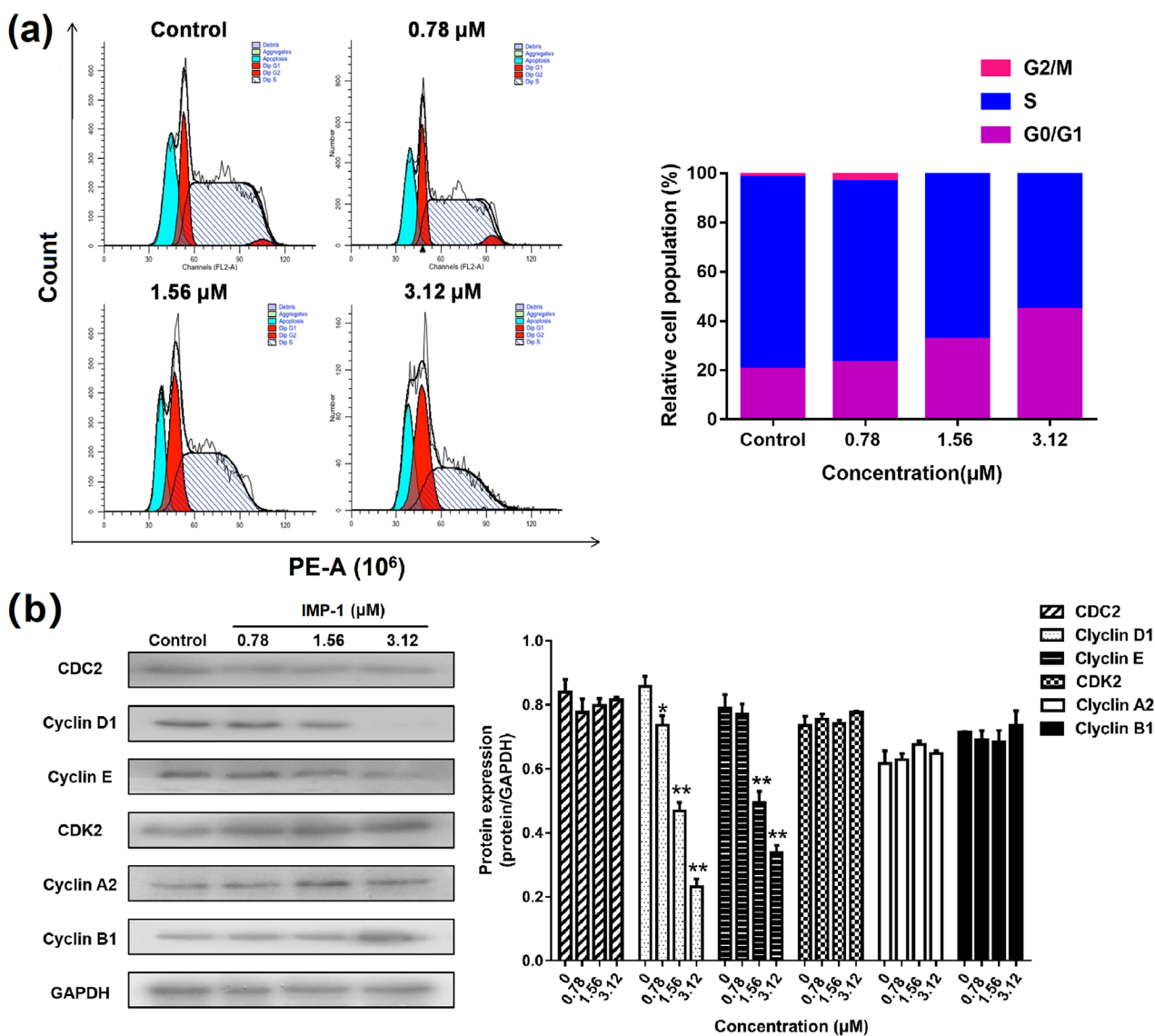


FIGURE 2 - Effect of IMP-1 on cell cycle distribution. (a) 786-O cells were treated with IMP-1 (0, 0.78, 1.56 and 3.12 μM) for 48 h followed by staining with propidium iodide for flow cytometric analysis. (b) Expression levels of CDC2, CDK2, Cyclin A2, Cyclin B1, Cyclin D1 and Cyclin E in 786-O cells treated with IMP-1 (0, 0.78, 1.56 and 3.12 μM) for 48 h were examined by western blot assay and the results were quantified by densitometry analysis of the bands and normalization to GAPDH. Data are presented as the mean standard error of the mean (n=3).

Effect of IMP-1 on cell apoptosis

In order to determine the effect of IMP-1 on cell apoptosis, 786-O cells were stained with Hoechst 33258 dye. As shown in Figure 3a, hoechst staining of 786-O cells indicated that IMP-1 induced an apoptotic event of chromatin condensation. Furthermore, the cells were stained with Annexin V-FITC and PI and analyzed by

flow cytometer to verify effect of IMP-1 on cell apoptosis. After treatment with IMP-1, the proportion of early and late apoptosis of 786-O cells increased significantly in a dose-dependent manner. The percentage of apoptotic cells was 2.76, 5.87, 17.71 and 26.33% in 786-O cells following treatment with IMP-1 (0, 0.78, 1.56 and 3.12 μM), respectively (Figure 3b).

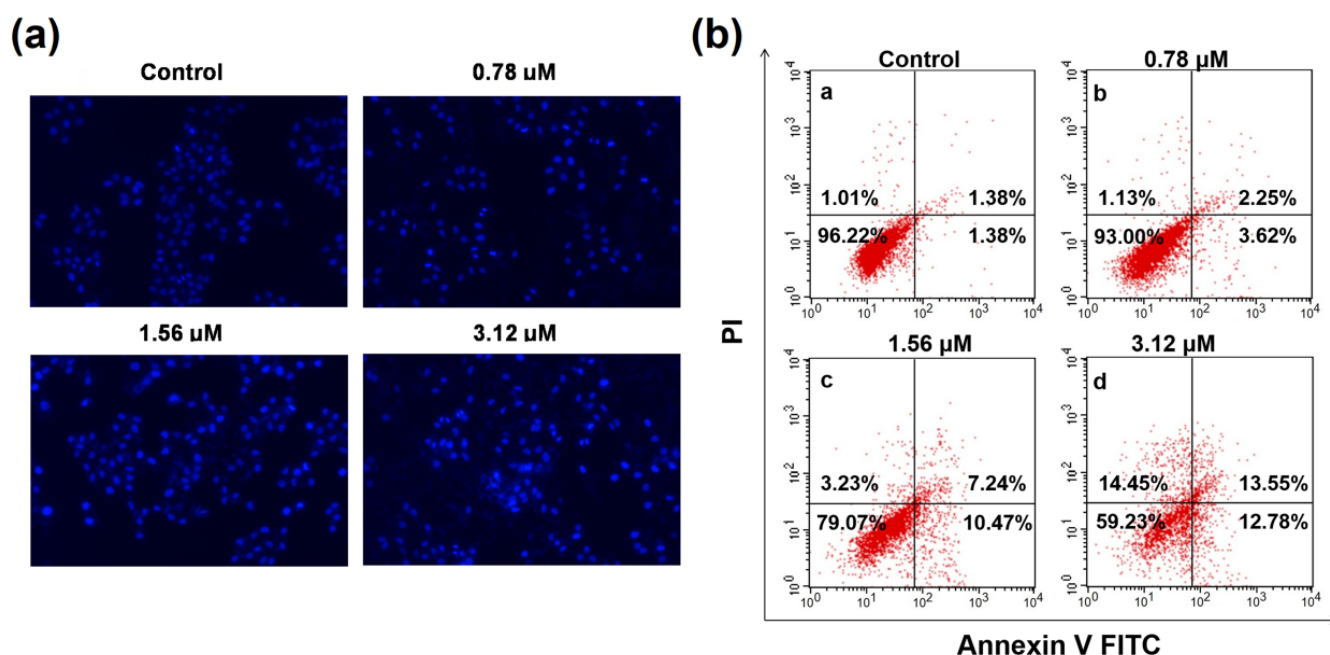


FIGURE 3 - Effect of IMP-1 on cell apoptosis. (a) IMP-1-induced apoptosis in 789-O cells were characterized by nuclear condensation or nuclear fragmentation after Hoechst staining. (b) Flow cytometric analysis of IMP-1-induced apoptosis in 789-O cells. The flow cytometry profile presents Annexin V FITC (x axis) and PI staining (y axis). The values represent the percentage of cells in each of the four quadrants (lower left quadrant, viable cells; upper left quadrant, necrotic or dead cells; lower right quadrant, early stage apoptotic cells; and upper right quadrant, late stage apoptotic cells).

$\Delta\psi_m$ was measured by flow cytometer to verify effect of IMP-1 on cell apoptosis. The percentage of 786-O cells exposed to IMP-1 revealed a notable decrease in Rhodamine 123 fluorescence intensity from 95.24% in control to 88.79%, 70.62% and 58.01%, respectively (Figure 4a).

Effect of IMP-1 on apoptosis regulatory molecules

The effect of IMP-1 on anti-apoptotic and pro-apoptotic proteins were investigated by western blot analysis. With the increase of concentration, IMP-1 significantly decreased the expression of mcl-1 and Bcl-2, and increased the expression of Bad, Bak and Bax (Figure 4b).

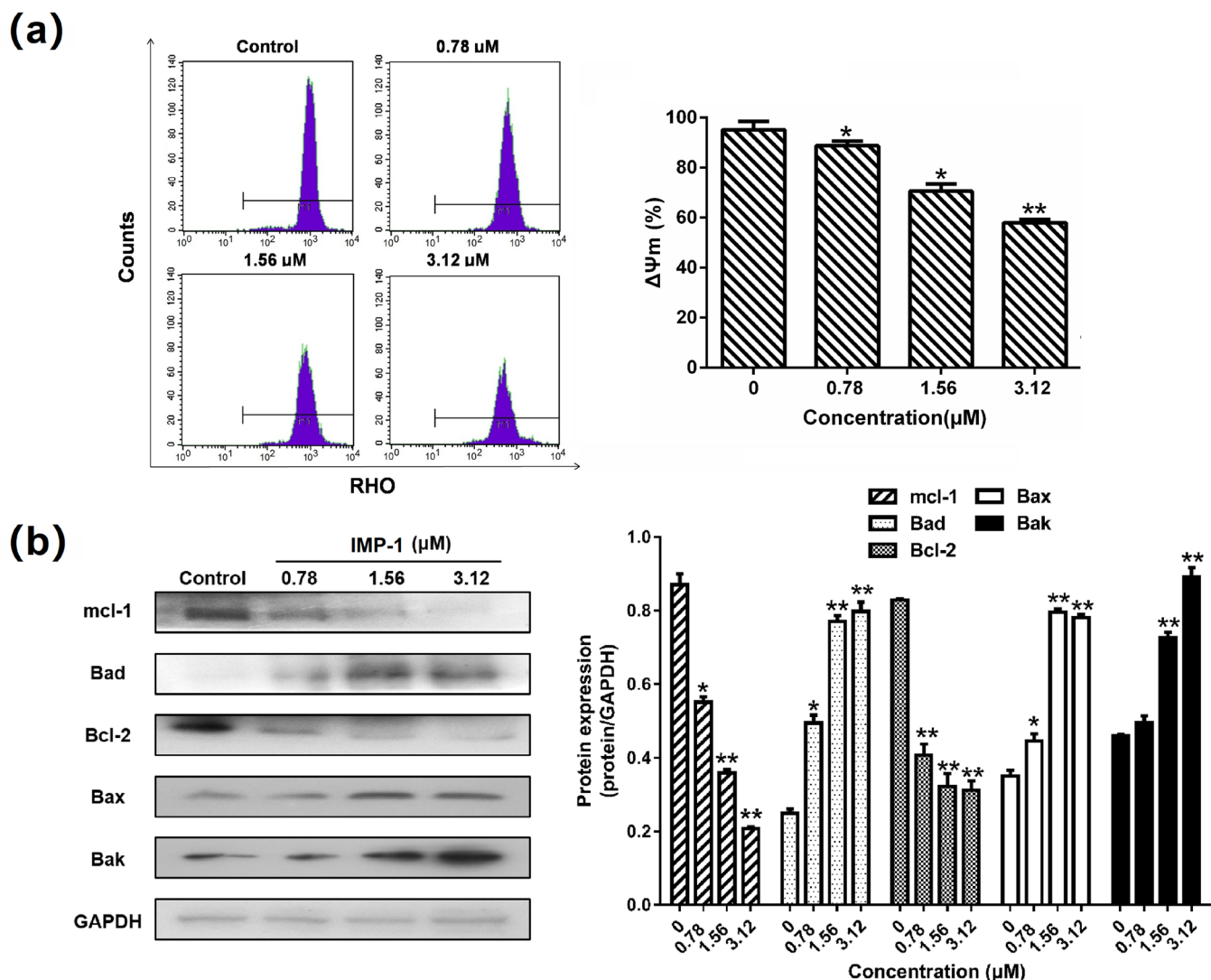


FIGURE 4 - The mechanism of IMP-1 on cell apoptosis. (a) The mitochondrial membrane potential ($\Delta\Psi_m$) were assessed using flow cytometry following treatment of the 786-O cells with IMP-1 (0.78, 1.56 or 3.12 μM) for 48 h. (b) Expression levels of Bad, Bak, Bax, Bcl-2 and Mcl-1 in 786-O cells treated with IMP-1 (0, 0.78, 1.56 and 3.12 μM) for 48 h were examined by western blot assay and the results were quantified by densitometry analysis of the bands and normalization to GAPDH. Data are presented as the mean standard error of the mean (n=3).

Effect of IMP-1 on EphrinB2 signaling pathway

In order to further clarify whether EphrinB2 was a key factor of IMP-1, the expression of EphrinB2 and its related proteins were investigated by western blot assay. The results showed that the mRNA and protein expression of EphrinB2 were strongly decreased by IMP-1 treatment (Figure 5a, b). To verify the key role of EphrinB2 in the effects induced by IMP-1, EphrinB2

was transiently knocked down in 786-O cells (786-O-KO) (Figure 5c). Results showed that knockdown of EphrinB2 decreased the inhibitory effect of IMP-1 in 786-O cell viability (Figure 5d). Meanwhile, EphrinB2 was transiently transfected in 786-O cells (Figure 5e), and the transfection of EphrinB2 enhanced the inhibitory effect of IMP-1 in 786-O cell viability (Figure 5f). These data verified the effect of IMP-1 on EphrinB2.

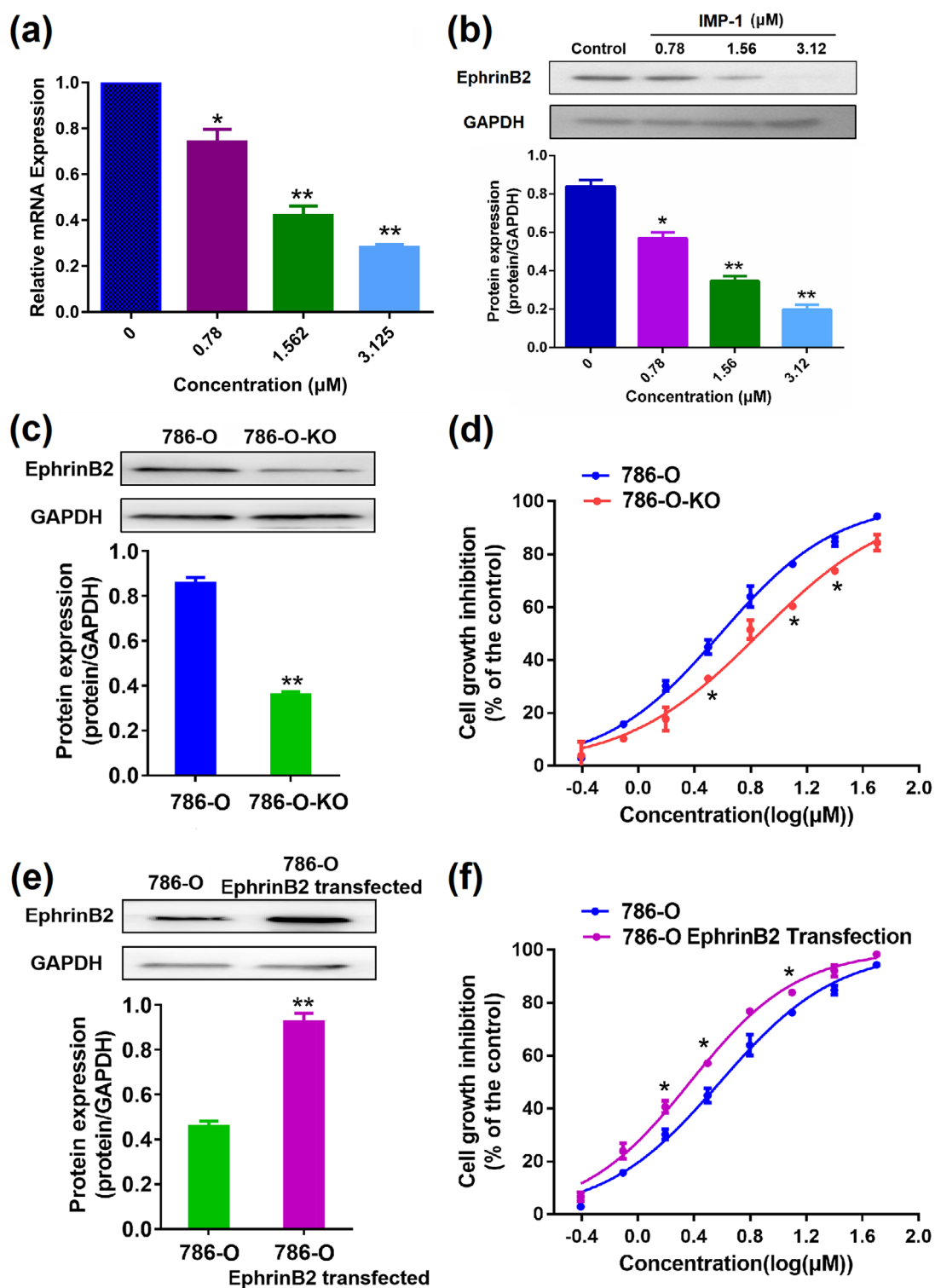


FIGURE 5 - Effect of IMP-1 on EphrinB2. (a) Expression level of EphrinB2 mRNA in 786-O cells treated with IMP-1 (0, 0.78, 1.56 and 3.12 μM) for 48 h were examined by PCR. (b) Protein level of EphrinB2 in 786-O cells treated with IMP-1 (0, 0.78, 1.56 and 3.12 μM) for 48 h were examined by western blot assay. (c) The expression of EphrinB2 on 786-O cells and 786-O-KO cells. (d) The effect of IMP-1 in inhibiting the growth of 786-O cells and 786-O-KO cells. **p*<0.05 versus the 786-O group. (e) The expression of EphrinB2 on 786-O cells and 786-O/EphrinB2 transfection cells. (f) The effect of ND-17 in inhibiting the growth of 786-O cells and 786-O/EphrinB2 transfection cells. **p*< 0.05 versus the 786-O group. Data are presented as the mean standard error of the mean (n=3).

Furthermore, the expression of its PDZ binding protein (Syntenin 1 and PICK1) were also decreased by IMP-1 treatment (Figure 6a). In addition, treatment of

IMP-1 significantly decreased the phosphorylation of Erk1/2 and AKT (Figure 6b).

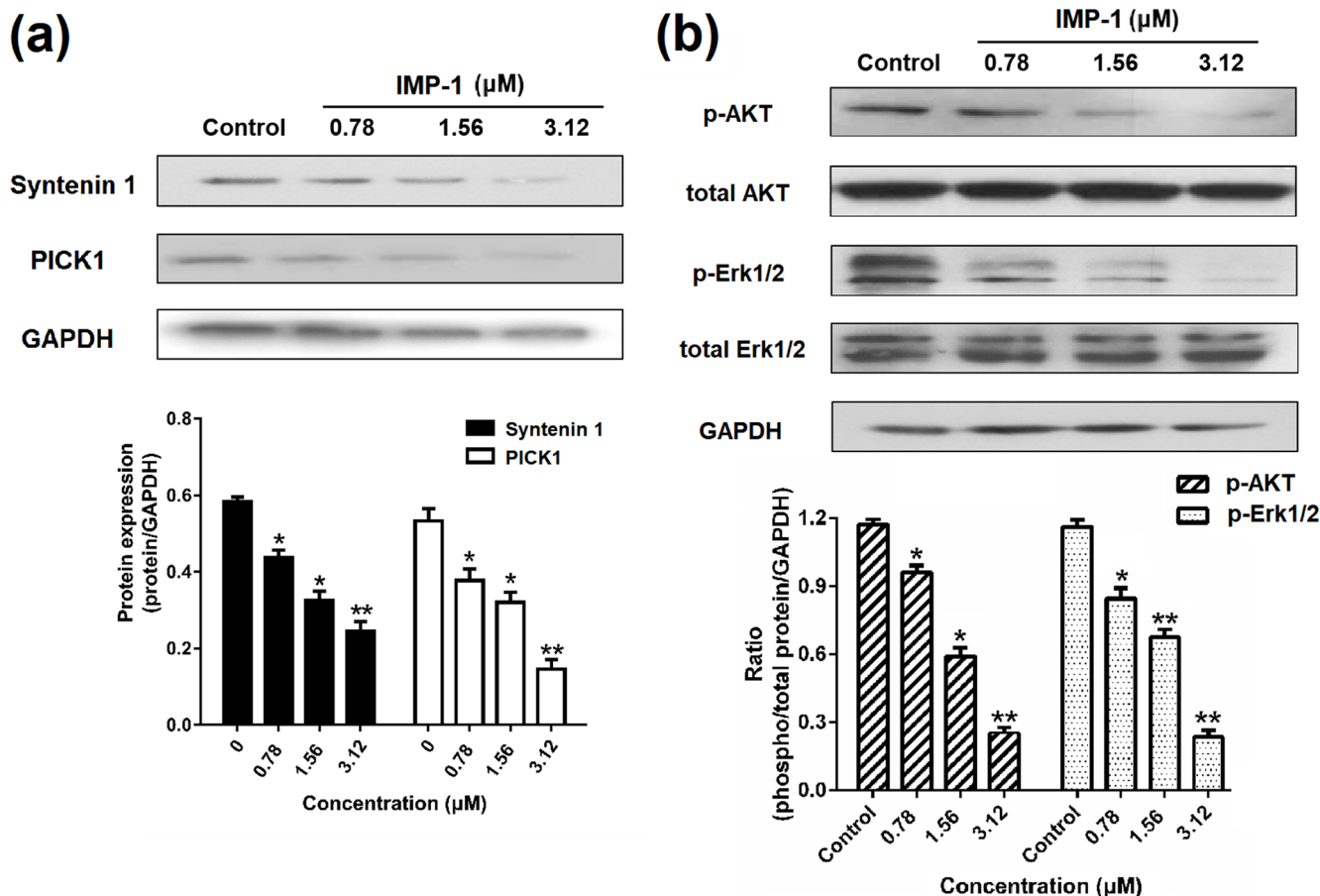


FIGURE 6 - Effect of IMP-1 on EphrinB2 signaling pathway. (a) Protein levels of Syntenin1 and PICK1 in 786-O cells treated with IMP-1 (0, 0.78, 1.56 and 3.12 μM) for 48 h were examined by western blot assay. (b) The phosphorylation of AKT and Erk1/2 in 786-O cells treated with IMP-1 (0, 0.78, 1.56 and 3.12 μM) for 48 h were examined by western blot assay. Data are presented as the mean standard error of the mean (n=3).

DISCUSSION

RCC is a common kidney cancer with an incidence rate as high as 85% (Barata, Rin, 2017). In this study, IMP-1 could inhibit the growth of RCC 786-O cells by regulating EphrinB2 signaling pathway. Results showed that IMP-1 could inhibit the 786-O cell proliferation in a dose- and time-dependent manner.

EphrinB2 plays a key role in tumor angiogenesis, metastasis and growth. The PDZ domain effector with Syntenin 1 and PICK1 is required for EphrinB2 to regulate the following signaling pathways. The results indicated that IMP-1 treatment could reduce the mRNA and protein levels of EphrinB2. More importantly, knockdown and transfection of EphrinB2 altered the inhibitory effect of IMP-1 in 786-O cell viability. These data indicated that IMP-1 inhibited 786-O cell growth via targeting

EphrinB2. In addition, the expression of PDZ binding proteins (Syntenin 1 and PICK1) was down-regulated by treatment of IMP-1 in 786-O cells. Furthermore, IMP-1 treatment significantly decreased the phosphorylation of Erk1/2 (MEK/ERK signaling member) and AKT (PI3K/AKT signaling member). It is well known that the mitogen-activated protein kinase MEK/ERK and PI3K/AKT cascades are commonly involved in cell growth, cell cycle and apoptosis (Zhang *et al.*, 2014).

The cell cycle includes interphases (G1, S, and G2 phases), and the mitotic (M) phase. The G1 phase is the stage of cells growth in preparation for DNA replication, and also the stage of determining whether the cells divide again or enter the quiescent G0 phase (Wenzel, Singh, 2018). We found that IMP-1 mediated 786-O cell growth by inducing partial G0/G1 phase cell cycle arrest. IMP-1 prevented cells from entering the S phase for DNA replication, and arrested cell cycle at the first checkpoints (R point).

In normal cell cycle, the progression of each cell cycle is tightly controlled by CDKs and Cyclins. Cyclin D1 is an important nuclear protein for cells to enter the G1 phase of the cell cycle. Cyclin E1-related kinase activity plays a key role in determining whether to initiate S phase (Kanska *et al.*, 2016). With IMP-1 treatment, the expressions of Cyclin D1 and Cyclin E were decreased in 786-O cells, indicating that some cells remained in G1 phase and could not enter S phase.

Apoptosis is a coordinated and usually energy-dependent process, involving the activation of a group of cysteine proteases called “cysteine proteases” and a complex cascade of events related to cell death (Elmore, 2007). In this study, results showed that the cells treated with IMP-1 exhibited the phenomenon of chromatin condensation. In addition, IMP-1 treatment led to a significant increase in the early- and late-stage apoptotic fractions in a dose-dependent manner. When cell apoptosis starts, the permeability of cell membrane changes, which is characterized by the destruction of $\Delta\psi_m$. $\Delta\psi_m$ reflects the functional state of mitochondria and is considered to be related to the differentiation state, tumorigenicity and malignancy (Zhang *et al.*, 2015). IMP-1 treatment led to a decrease of $\Delta\psi_m$, which further indicated that IMP-1 could induce cell apoptosis at early stage.

In order to further understand the mechanism of cell apoptosis induced by IMP-1, western blot was used to analyze its influence on the level of Bcl-2 family proteins. The role of the Bcl-2 family in cell apoptosis has long been confirmed. These proteins are divided into two subfamilies, such as anti-apoptotic proteins (Bcl-2, Mcl-1) and pro-apoptotic proteins (Bak, Bax, Bad), which play crucial roles in regulating mitochondrial-dependent apoptosis (Warren, Wong-Brown, Bowden, 2019). The current study detected the protein expression of Bcl-2, Mcl-1, Bak, Bax and Bad in 786-O cells using western blot analysis. The results showed that IMP-1 induced the down-regulation of Bcl-2 and Mcl-1 expression, and the up-regulation of Bak, Bax and Bad expression.

In conclusion, the present study demonstrated that IMP-1 could regulate the EphrinB2 signaling pathway in order to inhibit 786-O cell growth by arresting the cell cycle at the G0/G1 phase and inducing cell apoptosis. Therefore, IMP-1 may present a potential strategy for the treatment of RCC.

ACKNOWLEDGMENTS

None.

CONFLICT OF INTEREST

The authors declare that they have no conflict of interest.

DATA AVAILABILITY

The data used to support the findings of this study are included within the article.

REFERENCES

- Barata PC, Rini BI. Treatment of renal cell carcinoma: Current status and future directions. *CA Cancer J Clin.* 2017;67(6):507-524.
- Bonelli M, La Monica S, Fumarola C, Alfieri R. Multiple effects of cdk4/6 inhibition in cancer: From cell cycle arrest to immunomodulation. *Biochem Pharmacol.* 2019;170:113676.

- Curtis SA, Cohen JV, Kluger HM. Evolving immunotherapy approaches for renal cell carcinoma. *Curr Oncol Rep.* 2016;18(9):57.
- Dravis C, Henkemeyer M. Ephrin-b reverse signaling controls septation events at the embryonic midline through separate tyrosine phosphorylation-independent signaling avenues. *Dev Biol.* 2011;355(1):138-151.
- Elmore S. Apoptosis: A review of programmed cell death. *Toxicol Pathol.* 2007;35(4):495-516.
- Genander M, Frisen J. Ephrins and eph receptors in stem cells and cancer. *Curr Opin Cell Biol.* 2010;22(5):611-616.
- Germain S, Eichmann A. Vegf and ephrin-b2: A bloody duo. *Nat Med.* 2010;16(7):752-754.
- Gray RE, Harris GT. Renal cell carcinoma: Diagnosis and management. *Am Fam Physician.* 2019;99(3):179-184.
- He HZ, Wang C, Wang T, Zhou N, Wen ZY, Wang SC, et al. Synthesis, characterization and biological evaluation of fluorescent biphenyl-furocoumarin derivatives. *Dyes Pigm.* 2015;113:174-180.
- Kanska J, Zakhour M, Taylor-Harding B, Karlan BY, Wiedemeyer WR. Cyclin e as a potential therapeutic target in high grade serous ovarian cancer. *Gynecol Oncol.* 2016;143(1):152-158.
- Kozioł E, Skalicka-Woźniak K. Imperatorin-pharmacological meaning and analytical clues: Profound investigation. *Phytochem Rev.* 2016;15:627-649.
- Li J, Wang D, Liu J, Qin Y, Huang L, Zeng Q, et al. Rcel expression in renal cell carcinoma and its regulatory effect on 786-o cell apoptosis through endoplasmic reticulum stress. *Acta Biochim Biophys Sin.* 2017;49(3):254-261.
- Liu F, Wan L, Zou H, Pan Z, Zhou W, Lu X. Prmt7 promotes the growth of renal cell carcinoma through modulating the β -catenin/c-myc axis. *Int J Biochem Cell Biol.* 2020;120:105686.
- Ma W, Zhu M, Zhang D, Yang L, Yang TF, Li X, et al. Berberine inhibits the proliferation and migration of breast cancer zr-75-30 cells by targeting ephrin-b2. *Phytomedicine.* 2017a;25:45-51.
- Ma WN, Zhu M, Yang L, Yang TF, Zhang YM. Synergistic effect of tpd7 and berberine against leukemia jurkat cell growth through regulating ephrin-b2 signaling. *Phytother Res.* 2017b;31(9):1392-1399.
- Malumbres M, Barbacid M. Cell cycle, cdks and cancer: A changing paradigm. *Nat Rev Cancer.* 2009;9(3):153-166.
- Messeha SS, Zarmouh NO, Mendonca P, Alwagdani H, Cotton C, Soliman KFA. Effects of gossypol on apoptosis-related gene expression in racially distinct triple-negative breast cancer cells. *Oncol Rep.* 2019;42(2):467-478.
- Messeha SS, Zarmouh NO, Asiri A, Soliman KFA. Rosmarinic acid-induced apoptosis and cell cycle arrest in triple-negative breast cancer cells. *Eur J Pharmacol.* 2020;885:173419.
- Poliakov A, Cotrina M, Wilkinson DG. Diverse roles of eph receptors and ephrins in the regulation of cell migration and tissue assembly. *Dev Cell.* 2004;7(4):465-480.
- Posadas EM, Limvorasak S, Figlin RA. Targeted therapies for renal cell carcinoma. *Nat Rev Nephrol.* 2017;13(8):496-511.
- Warren CFA, Wong-Brown MW, Bowden NA. Bcl-2 family isoforms in apoptosis and cancer. *Cell Death Dis.* 2019;10(3):177.
- Wenzel ES, Singh ATK. Cell-cycle checkpoints and aneuploidy on the path to cancer. *In Vivo.* 2018;32(1):1-5.
- Wu KC, Chen YH, Cheng KS, Kuo YH, Yang CT, Wong KL, et al. Suppression of voltage-gated na(+) channels and neuronal excitability by imperatorin. *Eur J Pharmacol.* 2013;721(1-3):49-55.
- Zhang BB, Wang DG, Guo FF, Xuan C. Mitochondrial membrane potential and reactive oxygen species in cancer stem cells. *Fam Cancer.* 2015;14(1):19-23.
- Zhang YM, Zhan YZ, Zhang DD, Dai BL, Ma WN, Qi JP, et al. Eupolyphaga sinensis walker displays inhibition on hepatocellular carcinoma through regulating cell growth and metastasis signaling. *Sci Rep.* 2014;4:5518.
- Zhu M, Cui Y, Yang L, Yang T, Wang H, Zhang D, et al. Ephrin type-b receptor 4 affinity chromatography: An effective and rapid method studying the active compounds targeting ephrin type-b receptor 4. *J Chromatogr A.* 2018;1586:82-90.

Received for publication on 23rd February 2022
 Accepted for publication on 14th September 2022